

Photocatalyst-free photochemical deuteration via H/D exchange with D₂O

Received: 23 December 2024

Accepted: 27 June 2025

Published online: 22 July 2025



Ying Meng^{1,2,10}, Bei Shu^{1,2,10}, Jing Zhang^{1,2,10}, Heng Rao^{1,3}, Ziyuan Zhou⁴,
Zhiyuan Wang^{1,2}✉, Zhongyi Liu², Kangdong Liu^{1,5,6,7},
Yueteng Zhang^{1,6,7}✉ & Wei Wang^{1,8,9}

Deuterium labeling is increasingly important across scientific fields, from drug development to materials engineering, but current methods often require expensive catalysts. Here we demonstrate a simple, photocatalyst-free approach for incorporating deuterium into organic molecules using visible light. By employing common thiol compounds under mild blue-light irradiation (380–420 nm), we successfully modify two key chemical groups (formyl and α -amino) with high efficiency (up to 96% deuterium incorporation). This method eliminates the need for specialized PCs, significantly reducing costs and complexity. Surprisingly, we find that the system generates reactive intermediates (thiyl radicals and hydrogen atoms) through previously unrecognized light-activated pathways. These discoveries challenge conventional assumptions about photochemical deuteration and offer practical advantages for both laboratory research and industrial-scale production. Our results provide a more sustainable and scalable route to deuterated compounds while opening possibilities for light-driven chemistry without expensive catalysts. This work advances isotope labeling technology and suggests broader applications for simple, light-powered reactions in chemical synthesis.

Deuterium-labeled compounds nowadays serve as vital tools in various scientific disciplines from materials science to medicinal chemistry^{1–6}. The incorporation of deuterium into perovskite single crystals has been demonstrated to significantly enhance their performance in X-ray detection applications⁷. Deuteration of optoelectronic materials has been shown to improve their efficacy in X-ray analytical techniques⁸. Perdeuterated organic light-emitting diodes (OLEDs) exhibit superior quantum efficiencies and extended operational lifetimes compared to their protonated counterparts^{9,10}. Furthermore, isotopically enriched compounds serve as valuable tools for elucidating complex reaction

mechanisms, metabolic pathways, and molecular interaction dynamics⁶. Notably, deuterium labeling has been found to optimize the absorption, distribution, metabolism, and excretion (ADME) profiles of pharmaceutical compounds. This advancement has led to the successful clinical translation of deuterated drugs, exemplified by the FDA approval of Deutetrabenazine¹¹ in 2017 and subsequent authorization of Deucravacitinib¹² (Fig. 1a).

The rapidly growing demand for deuterated molecules has stimulated the investigation of practical and reliable tactics for constructing deuterated compounds and their key building blocks^{13–16}. In

¹State Key Laboratory of Metabolic dysregulation & the Prevention and Treatment of Esophageal Cancer; School of Basic Medical Sciences, Zhengzhou University, Zhengzhou, China. ²College of Chemistry, Henan Institute of Advanced Technology, Zhengzhou University, Zhengzhou, China. ³State Key Laboratory of Inorganic Synthesis and Preparative Chemistry, College of Chemistry, Jilin University, Changchun, China. ⁴National Cancer Center/National Clinical Research Center for Cancer/Cancer Hospital & Shenzhen Hospital, Chinese Academy of Medical Sciences and Peking Union Medical College, Shenzhen, China. ⁵China-US (Henan) Hormel Cancer Institute, Zhengzhou, China. ⁶Provincial Cooperative Innovation Center for Cancer Chemoprevention, Zhengzhou University, Zhengzhou, China. ⁷Cancer Chemoprevention International Collaboration Laboratory, Zhengzhou University, Zhengzhou, China. ⁸Department of Pharmacology & Toxicology, University of Arizona, Tucson, AZ, USA. ⁹Department of Chemistry & Biochemistry, University of Arizona, Tucson, AZ, USA. ¹⁰These authors contributed equally: Ying Meng, Bei Shu, Jing Zhang. ✉e-mail: wangzhiy@zzu.edu.cn; yuetengzhang@zzu.edu.cn

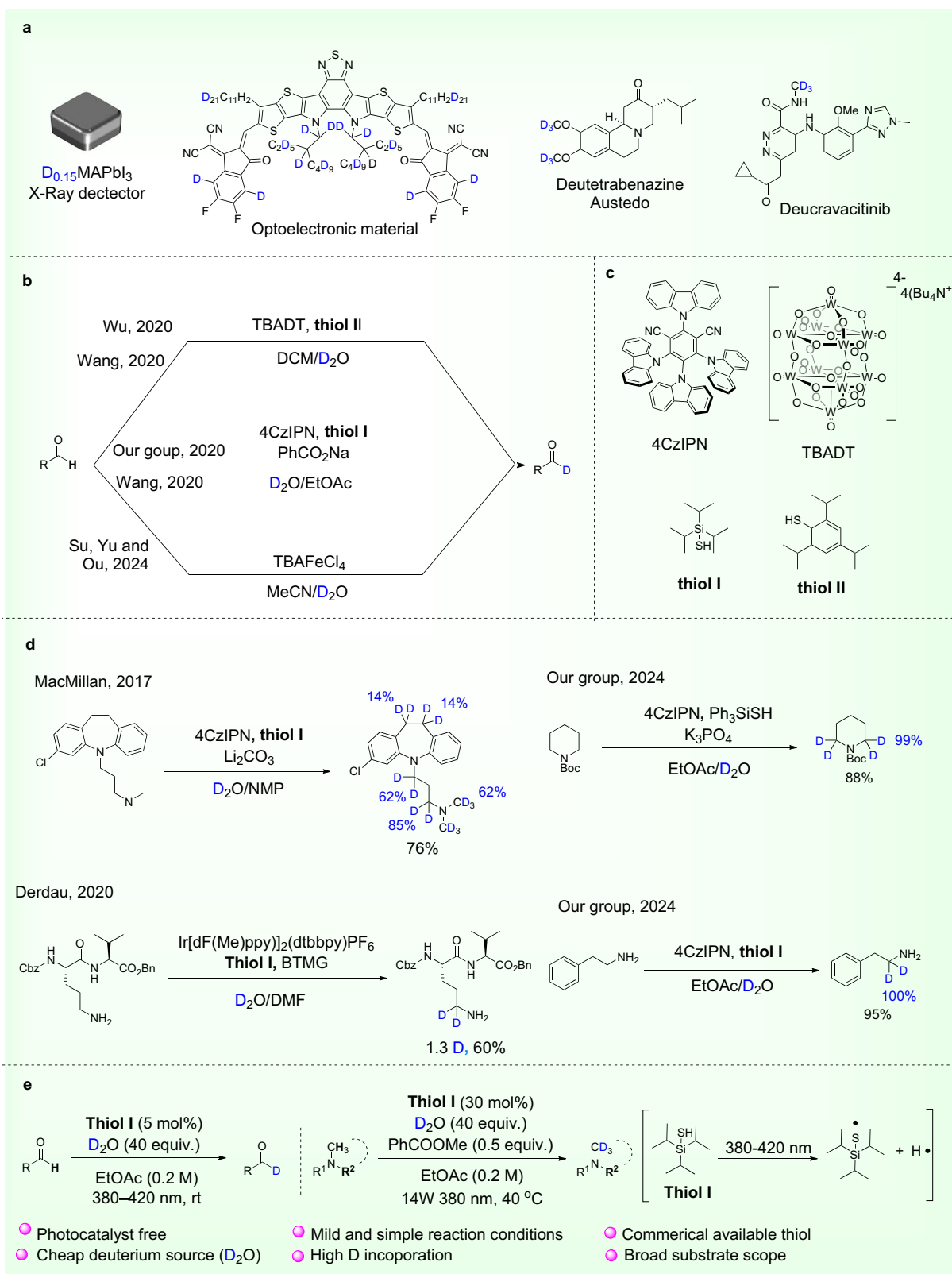


Fig. 1 | Deuterated compounds and deuteration methods. a Deuterated materials and drugs. **b** Deuteration of formyl group. **c** Deuteration of α -amines. **d** Photocatalyst and thiols. **e** Photocatalyst-free photocatalytic preparation of

deuterated aldehydes and α -amines via HDE (this work). HDE hydrogen-deuterium exchange, TBADT tetra-*n*-butylammonium decatungstate.

2017, MacMillan pioneered the photocatalyzed synthesis of deuterated pharmaceutical compounds, laying the foundation for the subsequent deuteration development¹⁷. Soon, Xie and co-workers systematically advanced this field by giving access to deuterated

aldehydes¹⁸ and alkanes^{19,20} based on their previous work²¹. Complementing these contributions, Studer achieved site-selective deuteration with high precision, catalyzed by AIBN. Moreover, Ye and coworkers realized the asymmetric synthesis of chiral deuterated

compounds assisted by chiral thiol^{22–24}. Within this area, synthetic strategies can be classified into reductive deuteration, dehalogenative deuteration, and hydrogen/deuterium exchange (HDE)^{25–31}. Benefit from the unchanged functional groups, HDE is regarded as the most efficient tactics^{20,32}. By taking advantage of the high-speed development of photochemistry, light-promoted HDE receives dramatic attention, generating various elegant methods for the deuteration of C(sp³)-H through radical process³³. The key steps generally involve the generation of carbon-centered radicals (C•) followed by deuterium D incorporation via a hydrogen atom transfer (HAT) process with a suitable D donor. The C• intermediates are typically formed through either proton-coupled electron transfer (PCET) or photocatalyst-mediated HAT. Additionally, in situ-generated thiol-d₁, produced via H/D exchange (HDE) with D₂O, commonly functions as the D donor to facilitate the deuteration step.

Aldehydes constitute a fundamental class of organic compounds that are not only prevalent in natural products but also serve as pivotal intermediates in chemical and pharmaceutical synthesis³⁴. Consequently, considerable research efforts, including those from our group, have been directed toward developing efficient and practical methodologies for the preparation of C-1-deuterated aldehydes^{35,36}. Among the diverse strategies explored, photocatalytic HDE of aldehydes has emerged as a particularly promising approach owing to its superior synthetic efficiency. To date, three principal photocatalytic systems have been reported for the activation of aldehyde C-H bonds to facilitate HDE: (1) a synergistic catalytic system comprising 4CzIPN and a thiol catalyst^{37,38}, (2) a cooperative system combining tetra-*n*-butylammonium decatungstate (TBADT) with a thiol catalyst^{39,40}, and (3) a single-component system utilizing solely TBAFeCl₄⁴¹ (Fig. 1b, c).

Amines represent another important class of compounds that are ubiquitously present in both natural products and pharmaceutical agents. However, the electron-rich character of nitrogen renders the α -position in drug molecules particularly susceptible to metabolic degradation, a limitation that can be effectively addressed through deuteration¹². Consequently, the development of efficient α -amine deuteration methodologies has attracted considerable research interest. To date, four distinct photocatalytic systems have been reported for the deuteration of tertiary, secondary, and primary amines. Building upon MacMillan's pioneering work, we have adapted a similar catalytic system for the deuteration of amides⁴² and primary amines⁴³. These reported methodologies employ a common strategy involving the synergistic combination of a photoredox catalyst with a thiol mediator (Fig. 1c, d). Notably, while α -deuteration of primary amines has been achieved using Ir[dF(Me)ppy]₂(dtbbpy)PF₆ as the photocatalyst, this approach currently suffers from limited deuterium incorporation efficiency⁴⁴.

Although numerous efficient HDE methodologies have been developed for the deuteration of formyl groups and α -amino positions, these reactions universally require noble-metal-based or organic photocatalysts (PCs). However, the reliance on PCs introduces additional challenges, including the costs associated with catalyst synthesis and the need for their subsequent removal during purification. Driven by the demand for a mild, selective, and photocatalyst-free (PC-free) HDE protocol, we propose a complementary strategy for site-selective deuteration that operates in the absence of PCs. This approach holds significant potential for broadening the applicability of deuteration reactions in both academic research and industrial applications.

To the best of our knowledge, PC-free deuteration methodology for organic compounds is rarely explored. It is well-established that thiyl radicals (S•) can abstract hydrogen atoms (H•) from C(sp³)-H bonds, yielding thiols and carbon-centered radicals (C•). Notably, thiols serve as excellent hydrogen atom donors due to their relatively weak S-H bonds (bond dissociation energy [BDE] \approx 87 kcal/mol) and favorable polarity-matching characteristics in radical reactions⁴⁵. The reversible nature of the interaction between S• and C-H bonds

suggests the theoretical feasibility of achieving C(sp³)-H deuteration through sustained thiyl radical generation in the presence of D₂O. Thiyl radicals can be generated via homolytic cleavage of S-H or S-S bonds, which can be induced either by radiolysis or high-energy light irradiation. Intriguingly, during our previous investigation into visible-light-mediated photocatalytic deuteration of formyl groups³⁸, we serendipitously observed that 4-methylbenzaldehyde underwent 85% deuteration after 24 h of 420 nm irradiation in the absence of any photocatalyst. This unexpected finding prompted us to explore the development of PC-free deuteration systems. Our experimental results demonstrate the viability of establishing a PC-free deuteration platform utilizing relatively low-energy light irradiation.

In this study, we present a PC-free light-mediated HDE methodology for formyl groups and α -amino C-H bonds in amines (Fig. 1e). This straightforward deuteration protocol facilitates the efficient synthesis of deuterated aldehydes and α -deuterated amines, achieving good to excellent yields (up to 99%) with high deuterium incorporation ratios (up to 96%), all in the absence of any photocatalyst.

Results

Reaction condition optimization for deuterating the formyl group

Building upon our expertise in deuteration chemistry, we initiated our investigation by examining the model deuteration reaction of *p*-tolualdehyde (**1a**) with D₂O in the presence of a HAT catalyst. Through systematic optimization of reaction parameters, we established the following optimal conditions: 5 mol% **thiol I** as HAT catalyst, 40 equivalents of D₂O in EtOAc at room temperature, under 380 nm irradiation for 12 h (Table 1, entry 1). These conditions afforded the desired product **2a** in 79% yield with excellent deuterium incorporation (94%). Notably, when employing 420 nm irradiation, the deuterium ratio decreased to 85% (entry 2), with further wavelength-dependent effects detailed in Supplementary Table 2. This phenomenon may be attributed to insufficient photon energy for efficient S-H bond dissociation at longer wavelengths. The selection of an appropriate thiol catalyst proved critical, as it must simultaneously fulfill two essential functions: serving as an effective hydrogen donor while generating a thiyl radical (S•) capable of efficient hydrogen abstraction. Comparative evaluation of various thiol derivatives revealed **thiol I** to be superior to both **thiol II** (entry 3) and **thiol III** (entry 4). The diminished performance of **thiol II** correlates with its relatively low S-H BDE = 80 kcal/mol⁴⁶, which compromises its hydrogen abstraction capability. Remarkably, we achieved a significant reduction in thiol loading from 30 mol% in our previous protocol to just 5 mol% in the current system while maintaining high deuteration efficiency (entry 5). This suggests that excessive thiol concentration may introduce competing hydrogenation pathways. However, further reduction to 1 mol% resulted in slightly diminished deuterium incorporation (87%, entry 6). Solvent screening studies demonstrated the superior performance of EtOAc compared to alternatives such as MeCN (72% D-incorporation, entry 7) and CHCl₃ (27%, entry 8). Additional ester solvents exhibited comparable efficacy (Supplementary Table 1, entries 9–11), highlighting the importance of solvent selection. Concentration studies revealed a modest negative correlation between dilution and deuteration efficiency (entry 9). Control experiments unequivocally confirmed the essential roles of both thiol catalyst and light irradiation in this transformation (entries 10 and 11).

Substrate scope study for aldehydes

Having established the optimized reaction conditions, we subsequently investigated the substrate scope by examining a diverse range of aromatic and aliphatic aldehydes (Fig. 2). This systematic exploration revealed that our deuteration protocol exhibits broad applicability, delivering excellent deuterium incorporation ratios with high regioselectivity. For aromatic aldehydes, the presence of methyl

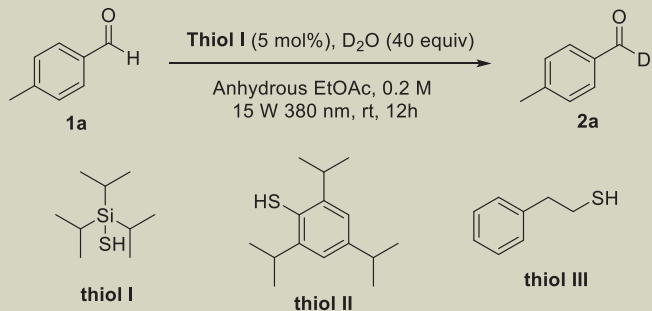
substituents at either *para*- (**2a**, 96% *D*) or *meta*-positions (**2b**, 92% *D*) of the phenyl ring did not significantly affect deuteration efficiency. The marginally reduced isolated yield for **2b** (66%) can be attributed to its relatively low boiling point, leading to partial loss during purification. Substrates bearing electron-donating groups, including MeO (**2c** **2f**), BnO (**2d**), PhO (**2e**), and OCH₂CH₂O (**2g**) moieties, were similarly compatible, affording moderate to excellent yields (51–99%) with substantial deuterium incorporation (82–90%). In contrast, electron-withdrawing substituents such as CN (**2h**) and COOMe (**2i**) groups led to complete consumption of starting materials under standard conditions, yielding instead benzoin and pinacol coupling products. This divergent reactivity can be rationalized by the lower S₁(n,π*) excited state energy of *p*-cyanobenzaldehyde (25950 ± 4 cm⁻¹, -385 nm) compared to *p*-methoxybenzaldehyde (27424 ± 26 cm⁻¹, -364 nm)⁴⁷. The electron-deficient nature of the cyano group facilitates photoexcitation at 380 nm, generating a reactive formal group diradical intermediate that undergoes subsequent dimerization. Notably, employing 420 nm irradiation successfully suppressed these side reactions while maintaining excellent deuteration efficiency (**2h**: 98% *D*, 71% yield; **2i**: 96% *D*, 61% yield). Halogen-substituted substrates (F: **2j**; Cl: **2k–l**; Br: **2m**) exhibited outstanding deuterium incorporation (91–97%), albeit with moderate yields (50–67%), again due to competing dimerization pathways. The protocol demonstrated remarkable functional group tolerance, accommodating ester (**2n–p**) and amide (**2q**) functionalities while maintaining high *D* ratios (92–96%). Particularly noteworthy was the hydroxyl-bearing substrate **2r**, which delivered near-quantitative yield (99%) with excellent deuteration (91%). Polyaromatic aldehydes, including 2-naphthaldehyde (**2s**) and 4-phenylbenzaldehyde (**2t**), despite their enhanced light absorption at 380 nm, showed minimal dimerization and provided good yields (68–85%) with high deuterium incorporation (87–90%). The methodology proved equally effective for heteroaromatic aldehydes (**2u–w**), demonstrating exceptional

regioselectivity by exclusively deuterating the formyl position while leaving metabolically labile α-amino positions (e.g., in **2v**) untouched. Aliphatic aldehydes, both primary (**2x–aa**) and secondary (**2ab**), were successfully deuterated with good efficiency. Remarkably, the system tolerated extended alkyl chains (e.g., 12-carbon in **2z**) and preserved the integrity of α-amino positions (**2ab**). The synthetic utility was further demonstrated through the deuteration of two pharmaceutical derivatives (**2ac**: 78% yield, 93% *D*; **2ad**: 48% yield, 94% *D*). To assess industrial applicability, we conducted gram-scale synthesis and D₂O recycling studies. Large-scale preparation of **2a** (1.07 g) maintained excellent performance (71% yield, 94% *D*). Moreover, recovered D₂O could be reused twice with only a marginal efficiency loss (2nd cycle: 79% yield, 91% *D*; 3rd cycle: 74% yield, 88% *D*). Finally, we confirmed the practicality of solar-driven deuteration, achieving 78% yield with 90% *D*-incorporation for **2a** under natural sunlight (Figs. 3 and Supplementary S12).

Deuteration of α-carbons of amines

Motivated by the successful development of an efficient and convenient protocol for formyl-d₁ aldehyde synthesis, we sought to extend this PC-free HDE methodology to other substrate classes. Given the fundamental importance of amines in natural products, pharmaceuticals, and as synthetic intermediates, coupled with the well-documented metabolic instability of α-amino carbon centers, we recognized the significant potential of applying our PC-free HDE approach to α-deuteration of nitrogen-containing compounds. Using *N*-methyldiphenylamine (**3a**) as a model substrate, initial investigations under conditions analogous to those employed for formyl deuteration afforded a modest 47% deuterium incorporation (Table 2, entry 1). Through systematic optimization of reaction parameters, we established the following optimal conditions: 30 mol% **thiol I-d1** as HAT catalyst, 0.5 equivalents of methyl

Table 1 | Exploration and optimization of reaction conditions

			
Entry	Variation of standard conditions	Yield (%) ^a	<i>D</i> ratio (%) ^b
1	None	92 (79 ^c)	94
2	420 nm instead of 380 nm	95	85
3	thiol II instead of thiol I	91	57
4	thiol III instead of thiol I	90	24
5	thiol I (30 mol%) instead of thiol I (5 mol%)	96	80
6	thiol I (1 mol%) instead of thiol I (5 mol%)	87	87
7	MeCN instead of EtOAc	96	72
8	CHCl ₃ instead of EtOAc	76	19
9	EtOAc (0.1 M) instead EtOAc (0.2 M)	89	93
10	Without thiol I	84	8
11	Without light	96	<5

^aYield was determined by ¹H NMR.

^b*D* ratio was determined by ¹H NMR.

^cIsolated yield.

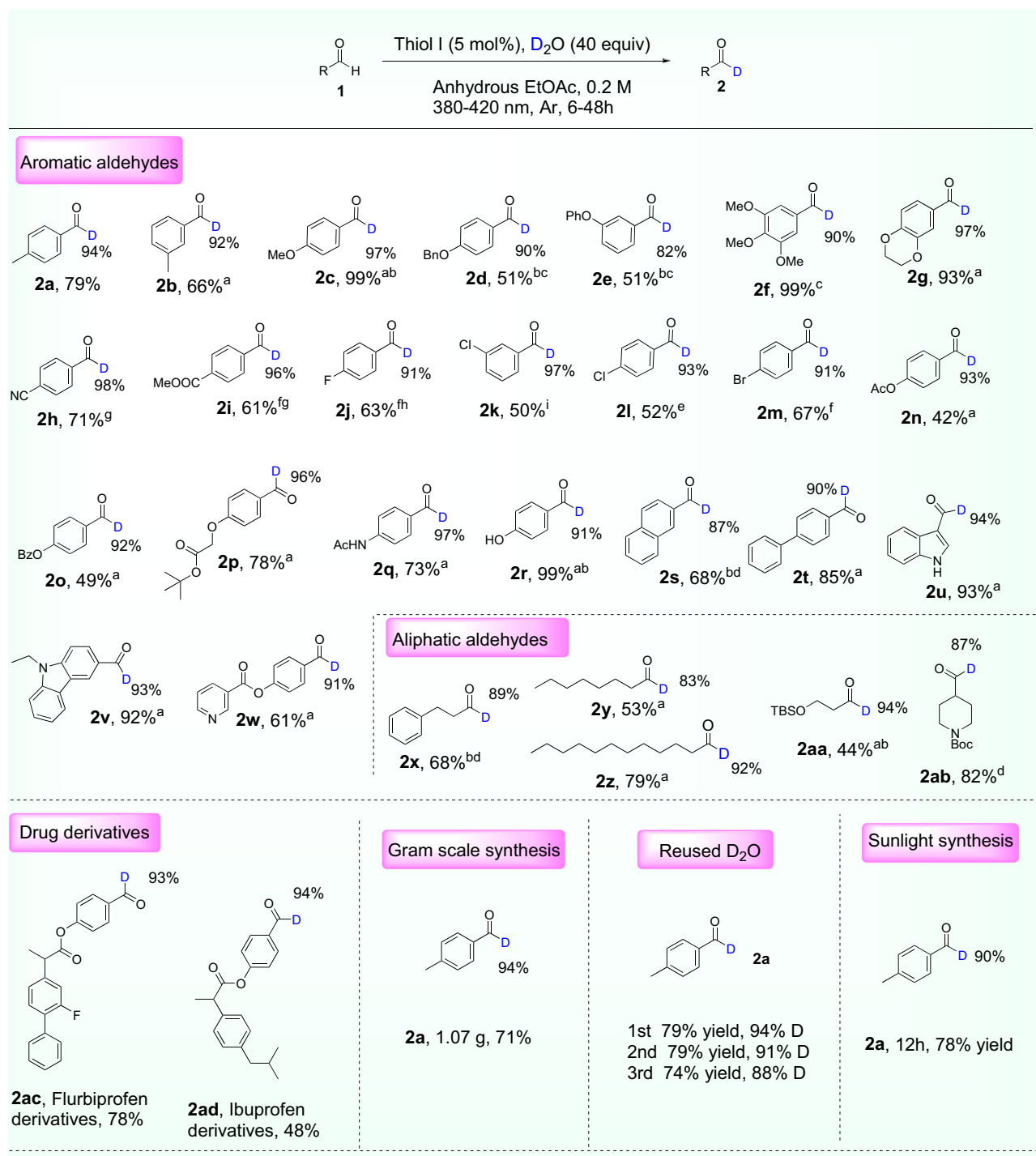


Fig. 2 | Substrate scope of aldehydes. ^a24h, ^b30 mol% **thiol I**, ^c48h, ^d36h, ^e2h, ^f10h, ^g420 nm, ^h400 nm, ⁱ1 h. Detailed procedure is seen in S8 in the Supplementary Information.

benzoate (PhCOOMe), and 40 equivalents of D₂O in EtOAc at room temperature under 380 nm irradiation for 24 h (entry 2). These conditions provided the desired product **4a** in near-quantitative yield (99%) with excellent deuterium incorporation (96%). Notably, methyl benzoate was serendipitously identified as a crucial additive for enhancing deuteriation efficiency. Consistent with our observations in formyl deuteriation, employing 420 nm irradiation resulted in reduced deuterium incorporation (85%, entry 3). Catalyst screening revealed the critical importance of **thiol I-d1**, as alternative HAT catalysts **thiol II** (<5%, entry 4) and **thiol III** (20%, entry 5) proved markedly less effective. The necessity of 30 mol% **thiol I-d1**

loading was further confirmed (entry 6), while solvent evaluation identified EtOAc as optimal (entries 7–9). Although acetonitrile afforded high deuterium incorporation (97%, entry 7), significant formation of *N*-methylcarbazole byproduct rendered it unsuitable. Interestingly, mild heating to 40 °C improved deuteriation efficiency by 5% compared to room temperature conditions (entry 10), while reduced reaction time led to diminished incorporation (entry 11). Counterintuitively, increasing D₂O equivalents to 100 resulted in lower deuteriation efficiency (entry 12). Control experiments confirmed the absolute requirement for both light irradiation and thiol catalyst (entry 13).

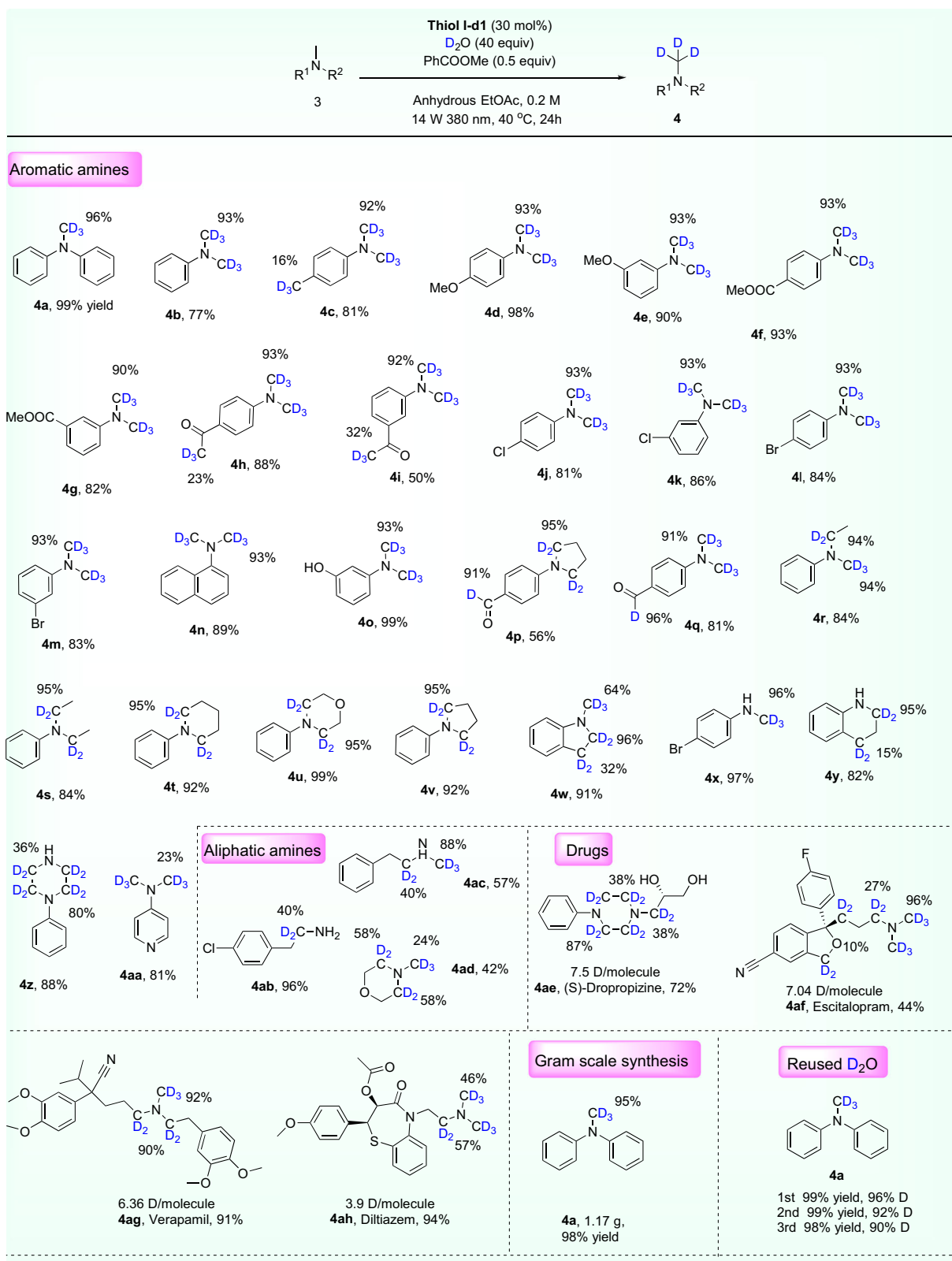


Fig. 3 | Substrate scope of amines. The detailed procedure is seen in S9 in the supplementary information.

Subsequently, we systematically examined the scope of α -carbon deuteration in nitrogen-containing compounds with respect to functional group tolerance and structural diversity. A broad range of amine substrates encompassing varied electronic properties and substitution patterns proved compatible with our deuteration protocol (Fig. 3). Beyond the monomethylated model substrate, *N,N*-dimethylaniline

derivatives (**4b–4c**) exhibited efficient deuteration of both methyl groups with excellent yields. The methodology accommodated diverse aromatic substituents, including electron-donating (MeO: **4d–4e**), electron-withdrawing (COOMe: **4f–4g**), and halogen (**4j–4m**) functionalities. Notably, polyaromatic systems (**4n**) and hydroxyl-containing substrates (**4o**) maintained high deuteration efficiency. As

Table 2 | Optimization of reaction conditions for deuterating α -amines

Entry	Variation of standard conditions	Yield (%) ^a	D ratio (%) ^b
1	Without PhCOOMe	98	47
2	None	99(99 ^c)	96
3	420 nm instead of 380 nm	96	85
4	thiol II instead of thiol I-d1	96	<5
5	thiol III instead of thiol I-d1	97	20
6	thiol I-d1 (15 mol%) instead of thiol I-d1 (30 mol%)	96	87
7	MeCN instead of EtOAc	18	97
8	CHCl ₃ instead of EtOAc	91	22
9	Toluene instead EtOAc	98	20
10	20 °C instead of 40 °C	97	91
11	12 h instead of 24 h	98	63
12	100 equiv of D ₂ O instead of 40 equiv	96	93
13	Without thiol I-d1 or light	99	<5

^aYield was determined by ¹H NMR.^bD ratio was determined by ¹H NMR.^cIsolated yield.

anticipated, formyl groups in **4p** and **4q** were simultaneously deuterated with high incorporation ratios. The protocol extended beyond methyl groups to successfully incorporate deuterium at α -positions of ethyl substituents (**4r–4s**). Various nitrogen heterocycles, including pyrrolidine (**4p–4v–4w**), piperidine (**4t**), morpholine (**4u**), and piperazine (**4z**) derivatives, demonstrated excellent deuterium incorporation. Intriguingly, while α -oxygen positions remained unaffected (**4u**), benzylic deuteration occurred in **4w** (32%) and **4y** (15%), likely attributable to the elevated electron density of the aromatic systems (see mechanistic discussion). Secondary aromatic amines (**4x–4y**) exhibited comparable deuteration efficiency to their tertiary counterparts. However, dimethylpyridine (**4aa**) showed markedly reduced incorporation (23%), suggesting potential electronic or coordination effects. Alkyl amines (**4ab–4ad**) displayed diminished deuteration efficiency, possibly reflecting substrate-dependent oxidation potentials. The synthetic utility was further demonstrated through the successful late-stage deuteration of pharmaceutical compounds, including (*S*)-Dropropizine (**4ae**), Verapamil (**4af**), Escitalopram (**4ag**), and Diltiazem (**4ah**), achieving up to 96% deuterium incorporation at α -amino positions. To assess industrial applicability, we conducted gram-scale synthesis and D₂O recycling studies analogous to our formyl deuteration investigations. Large-scale preparation of **4a** (1.17 g) maintained excellent efficiency (98% yield, 95% *D*). Remarkably, recovered D₂O retained high effectiveness upon reuse (2nd cycle: 99% yield, 92% *D*; 3rd cycle: 98% yield, 90% *D*; Fig. 4 and Supplementary S12).

To further explore the substrate scope of our deuteration protocol, we extended our investigation to additional functional classes, including ketones (acetophenone), alkenes (4-methylstyrene), and nitrogen-containing heterocycles (pyridine and carbazole). However, under the standard reaction conditions, no detectable deuterium incorporation was observed for these substrates. Notably, we identified modest but measurable deuteration at benzylic positions in compounds **4x** (32% *D*) and **4z** (15% *D*). This unexpected yet potentially valuable side reactivity may warrant further optimization in future studies to enhance both selectivity and efficiency for benzylic C–H bond deuteration.

Building upon the successful development of this PC-free deuteration methodology for formyl groups and amines, we proceeded to elucidate the underlying reaction mechanism. Control experiments employing TEMPO as a radical scavenger completely inhibited deuteration in both aldehyde and amine substrates (Fig. 4a, b), strongly suggesting a radical-mediated pathway. High-resolution mass spectrometry (HRMS) analysis of the reaction mixtures revealed the expected trapping products of acyl, α -amino, and thiyl radicals by TEMPO (Fig. 4a, b). Intriguingly, we also detected TEMPO–H adducts, indicating the presence of hydrogen atoms during the reaction process. To further investigate this observation, we examined the system for potential hydrogen gas evolution. Gas chromatography analysis confirmed the formation of H₂ under standard reaction conditions (Fig. 4d, e), a remarkable finding given the absence of any photocatalyst that could facilitate water splitting. This prompted us to

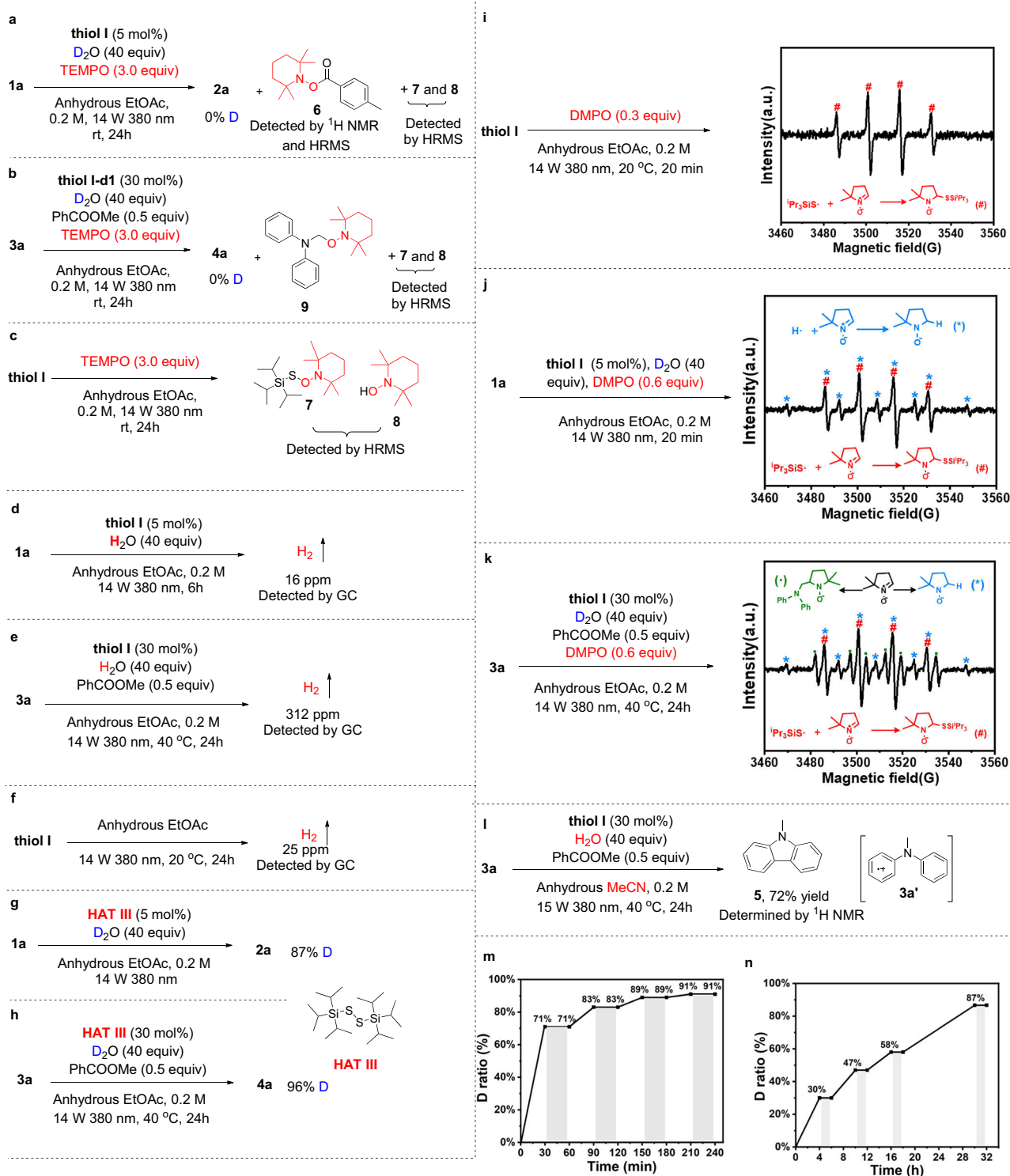


Fig. 4 | Mechanism study of deuterating formyl groups and α-amines. a Radicals trapped by TEMPO in the deuteriation of the formyl group. **b** Radicals trapped by TEMPO in the deuteriation of α-amines. **c** Radicals trapped by TEMPO in irradiation of thiol **I**. **d** H₂ gas analysis in deuteriation of aldehydes. **e** H₂ gas analysis in deuteriation of α-amines. **f** H₂ gas analysis in irradiation of thiol **I** in EtOAc.

g Deuteriation of aldehydes with disulfide as additive. **h** Deuteriation of α-amines with disulfide as additive. **i** EPR analysis in irradiation of thiol **I** in EtOAc. **j** EPR analysis in deuteriation of aldehydes. **k** EPR analysis in deuteriation of α-amines. **l** Byproduct *N*-Methylcarbazole detection. **m** ON/OFF experiment for deuteriation of aldehydes. **n** ON/OFF experiment for deuteriation of α-amines.

consider alternative hydrogen atom sources, leading us to hypothesize that homolytic cleavage of the relatively weak S–H bond (BDE ≈ 88 kcal/mol) in the thiol catalyst might occur under 380 nm irradiation. Subsequent TEMPO trapping experiments conducted with thiol in anhydrous ethyl acetate under 380 nm irradiation unequivocally demonstrated the generation of both TEMPO–H adducts (Fig. 4c) and

H₂ gas (Fig. 4f). These results provide direct evidence for the photolytic dissociation of S–H bonds under our reaction conditions, yielding thiol radicals and hydrogen atoms. The thiol radicals thus generated can abstract hydrogen atoms from relatively weak C–H bonds (e.g., formyl C–H) in the substrate. This mechanistic proposal is further supported by the comparable efficiency observed when using disulfide

catalysts (Fig. 4g, h), where the weaker S–S bond (compared to S–H) undergoes facile homolytic cleavage even at ambient temperature. To obtain more direct evidence for radical intermediates, we conducted electron paramagnetic resonance (EPR) spectroscopy experiments. As shown in Fig. 4i–k, we successfully detected characteristic signals corresponding to thiyl radical-DMPO spin adducts under three different reaction conditions^{48–51}. Complementary density functional theory (DFT) calculations were performed to evaluate the HAT process between thiyl radicals and *p*-tolualdehyde. The computed Gibbs free energy barrier for the transition state (**TS-2**) was found to be 15.54 kcal/mol (Fig. 5a), consistent with the observed reactivity at room

temperature. This energy barrier is reasonable considering the comparable BDE of the formyl C–H bond (≈88 kcal/mol in benzaldehyde)⁵² and the S–H bond in (*i*-Pr)₃SiSH (88.2 kcal/mol)⁵³. The similar BDE values, coupled with favorable polarity matching, enable the reversible hydrogen exchange between thiyl radicals and formyl groups. The proposed mechanism involves initial formation of (*i*-Pr)₃SiSD through HDE between (*i*-Pr)₃SiSH and D₂O, followed by subsequent deuterium transfer to the acyl radical intermediate. Light-on/off experiments (Fig. 4m, n) confirmed that this process does not proceed via a radical chain mechanism, but rather requires continuous irradiation to sustain the catalytic cycle.

Regarding the deuteration of α-amino compounds, our mechanistic investigations and prior studies suggest an analogous pathway to that observed in formyl group deuteration^{38,42,43}. To substantiate this hypothesis, we performed DFT calculations to examine the critical HAT step between the thiyl radical and *N*-methylphenylamine. The computed Gibbs free energy of the transition state (**TS-5**) was determined to be 16.44 kcal/mol (Fig. 5b), indicating that the HAT process is thermodynamically favorable under ambient conditions. Furthermore, complementary DFT calculations involving tertiary alkylamine substrates yielded comparable results (Supplementary Fig. 9a), providing additional support for the proposed mechanism.

Nevertheless, the potential involvement of a PCET mechanism between thiyl radicals and amines cannot be entirely excluded. As evidenced by the BDEs presented in Table 3 (entries 1–5), the α C–H bonds of nitrogen-containing compounds typically exhibit BDE values around 92 kcal/mol, significantly higher than the S–H BDE (88.2 kcal/mol) in (*i*-Pr)₃SiSH. This thermodynamic discrepancy suggests that direct HAT from amines to thiyl radicals is energetically disfavored. Given the electron-rich nature of *N,N*-dimethylaniline, and its facile oxidizability, we propose that the HDE in amines may alternatively proceed through a redox-mediated pathway. Comparative analysis of reduction potentials (Table 3, entries 5–10) reveals that aromatic amines (0.84 V, 0.71 V) demonstrate substantially lower oxidation potentials than their alkylamine counterparts (0.95 V, 1.1 V, and 1.36 V), correlating well with the observed deuteration efficiencies. This electrochemical trend is further supported by experimental results, where aromatic amines (e.g., **4b**, 93% D) consistently outperform aliphatic amines (e.g., **4ac**, 40% D) in deuteration efficiency. While thiyl radicals are conventionally recognized as hydrogen abstractors, they also exhibit significant oxidative capacity. The standard reduction potential of HOCH₂CH₂S• (+1.33 V vs SCE)⁵⁴, for instance, is sufficiently positive

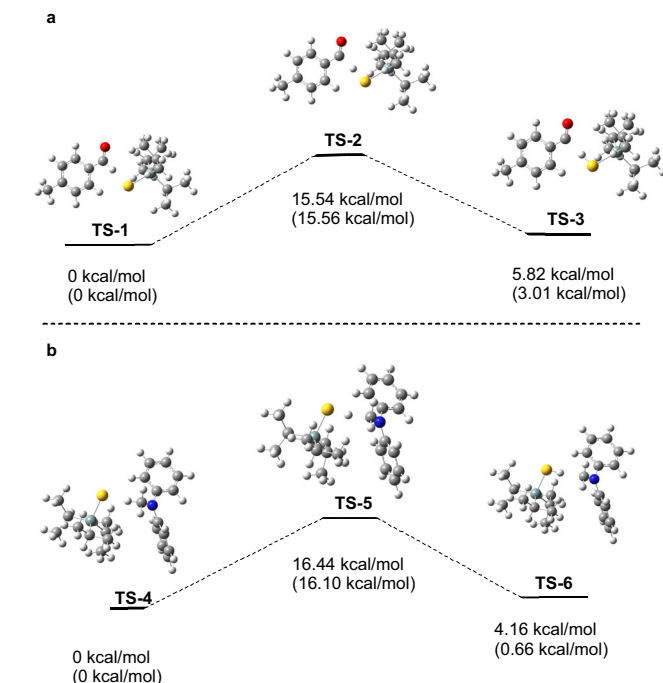


Fig. 5 | DFT calculation for transition states for the key step. a Gibbs energy of transition states in the reaction between thiyl radical and *p*-Methylaldehyde. **b** Gibbs energy of transition states in the reaction between thiyl radical and *N*-methylphenylamine. Values presented in brackets are single-point energy calculation results, which were conducted using the B3LYP/6-31G(d) optimized geometries with DFT B3LYP/6-31++G(d, p) basis set.

Table 3 | BDE of C–H bond and E_{red} of amines

Entry	Bond	BDE ⁵² (kcal/mol)	Entry	Compound	E_{red} (V)
1		90.6	6		0.84 ⁵⁶
2		91.6	7		0.71 ⁵⁶
3		89.9	8		0.95 ⁵⁷
4		91.8	9		1.1 ⁵⁷
5		92.6	10		1.36 ⁵⁷

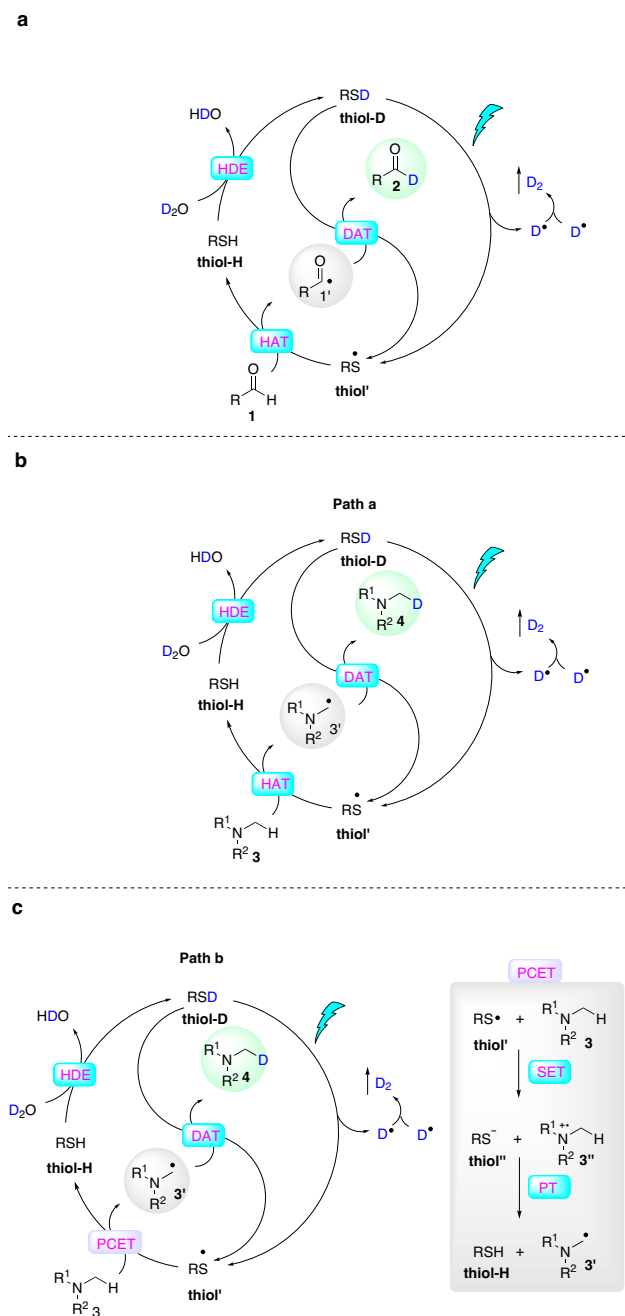


Fig. 6 | Proposed mechanism for deuteration. **a** Proposed mechanism for the deuteration of the formyl group. **b** Proposed mechanism (Path a) for deuteration of α -amines. **c** Proposed mechanism (Path b) for deuteration of α -amines.

to oxidize most amine substrates. This oxidative pathway is corroborated by the formation of *N*-methylcarbazole byproduct (Fig. 4l), which presumably originates from the delocalization of radical cation intermediates in the aromatic system (3a')⁵⁵. The observed benzylic deuteration in compounds **4x** (32% D) and **4z** (15% D) suggests that radical cation delocalization may enhance the acidity of benzylic protons, potentially facilitating their deprotonation to form benzylic radicals. Furthermore, the markedly reduced deuteration efficiency (23%) observed in electron-deficient substrate **4ab** underscores the critical influence of electronic effects on reaction kinetics. Collectively, these observations suggest that α -amino radicals may be generated via a PCET mechanism, despite the lack of supporting evidence from DFT calculations (Supplementary Fig. 9b). Following

radical formation, deuterium incorporation would then proceed analogously to the formyl deuteration pathway, involving HDE between the α -amino radical and (*i*-Pr)₃SiSD to yield the desired α -deuterated amine products.

Based on comprehensive mechanistic investigations, we propose the reaction pathway for the PC-free hydrogen-deuterium exchange (HDE) of formyl groups as illustrated in Fig. 6a. The catalytic cycle initiates with in situ HDE between thiol-H and D₂O, generating thiol-D. Subsequent photolytic homolytic cleavage of thiol-D under irradiation yields a thiyl radical (S•) and a D atom, with the latter potentially recombining to form D₂ gas. The thiyl radical then abstracts a hydrogen atom from the formyl group of aldehyde substrate **1** via a HAT pathway, producing an acyl radical intermediate **1'** while regenerating thiol-H. Finally, deuterium atom transfer (DAT) between the acyl radical **1'** and thiol-D affords the deuterated aldehyde product **2**, concurrently regenerating the thiyl radical to perpetuate the catalytic cycle.

For the α -amine deuteration process, we have identified two plausible mechanistic pathways (Fig. 6b, c). Pathway **a** (Fig. 6b) follows an analogous mechanism to the formyl deuteration: (1) photolytic cleavage of thiol-D generates thiyl radical and deuterium atom; (2) HAT between the thiyl radical and amine substrate produces an α -amino radical while reforming thiol-H; and (3) subsequent DAT between the α -amino radical and thiol-D yields the desired α -deuterated amine product while regenerating the thiyl radical catalyst. Alternatively, pathway **b** (Fig. 6c) involves a distinct redox-mediated mechanism: (1) single-electron oxidation of the amine substrate **3** by the thiyl radical generates a radical cation intermediate **3''** and a sulfur-centered anion **thiol''**; (2) proton transfer from the radical cation to the sulfur anion forms thiol-H and an α -amino radical **3'**; and (3) DAT between this radical intermediate and thiol-D then produces the deuterated amine product **4** while regenerating the thiyl radical. This oxidative pathway is particularly favored for electron-rich aromatic amines, as supported by our electrochemical studies. Both pathways ultimately lead to progressive deuterium incorporation through continuous catalytic cycling.

This study revealed the critical role of EtOAc as the optimal solvent, as alternative non-ester solvents, including MeCN and CHCl₃, demonstrated substantially lower deuteration efficiency. We postulate that hydrogen bonding interactions between the thiol catalyst and EtOAc may facilitate the photolytic cleavage of the S–H bond. DFT calculations support this hypothesis, demonstrating that hydrogen bond formation with EtOAc elongates the S–H bond length from 1.35083 Å to 1.35338 Å (Supplementary Fig. 10b). By comparison, MeCN forms weaker hydrogen bonding with S–H than that with EtOAc, and CHCl₃ provides even less activation effect (Supplementary Fig. 10c, d). These computational findings are consistent with experimental results (Table 1, entries 7–8) and provide compelling evidence for the crucial solvent effect observed in our deuteration system.

From an environmental sustainability perspective, our PC-free methodology offers significant advantages over conventional approaches. Previous deuteration methods typically employed noble metal complexes (e.g., Ir-based catalysts) or organic dyes (e.g., 4CzIPN) as PCs. The environmental impact of iridium mining includes substantial ecological damage through land degradation, water contamination, and atmospheric pollution resulting from open-pit excavation, chemical leaching processes, and particulate emissions. Furthermore, iridium extraction is both energy- and resource-intensive, generating considerable greenhouse gas emissions and toxic byproducts such as cyanide compounds. While organic PCs present reduced environmental burdens in terms of toxicity and energy requirements during synthesis and application, our catalyst-free system represents a further advancement by completely eliminating the need for these materials.

Table 4 | Comparison of this study with other photocatalytic HDE methods

Comparison of this study with other photocatalytic HDE methods for the formyl group					
Methods	Wang, 2020 ³⁹	Wang, 2020 ³⁸	Wang, 2021 ³⁷	Su, Yu, Ou, 2024 ⁴¹	This work
Catalyst	TBADT	4CzIPN	4CzIPN	TBAFeCl ₄	None
Yield (%)	73–95	50–99	49–93	55–90	41–99
D incorporation (%)	87–96	90–98	90–99	87–99	82–97
Reaction time	24 h–4 days	36 h	36 h	12–48 h	6–48 h
Light intensity and wavelength	36 W, 390 nm	5 W, blue light	36 W, blue light	40 W, 390 nm	14 W, 380 nm
Comparison of this study with other photocatalytic HDE methods for α -amines					
Methods	MacMillan, 2017 ¹⁷	Wang, 2024 ⁴³	Wang, 2024 ⁴²	This study	
Catalyst	Ir(F-Meppy) ₂ (dtbbpy)PF ₆ or 4CzIPN	4CzIPN	4CzIPN	None	
Yield (%)	59–88	80–98	80–92	57–99	
D incorporation (%)	27–90	85–100	76–100	23–96	
Reaction time	24 h	48 h	48 h	24–48 h	
Light intensity and wavelength	34 W, blue light	Two 40 W, blue light	Two 40 W, blue light	14 W, 380 nm	
Substrates	Tertiary amines	Primary aliphatic amines	Amides	Tertiary and secondary amines	

Comparative analysis with existing photocatalytic HDE methodologies reveals both advantages and limitations of our approach (Table 4). For formyl group deuteration, our protocol achieves comparable yields and deuterium incorporation ratios while requiring shorter reaction times for certain substrates. In the case of amine deuteration, similar efficiencies and reaction times are observed relative to established methods, with the additional benefit of reduced light intensity requirements. However, it should be noted that the current methodology is primarily applicable to secondary and tertiary amines, demonstrating limited efficacy for primary amines and amide functionalities.

Discussion

In this study, we report a PC-free photochemical strategy for the site-selective deuteration of aldehydes and amines. Utilizing commercially available thiols—either alone or in combination with methyl benzoate as an additive—in the presence of D₂O under 380–420 nm irradiation, we achieved high yields and excellent deuterium incorporation (up to 96%) for both Cl-deuterated aldehydes and α -deuterated amines. The broad applicability of this method is demonstrated by its successful implementation across aromatic, aliphatic, and drug-derived substrates. Moreover, the operational simplicity, mild reaction conditions, and cost-effective use of D₂O as the deuterium source highlight the potential for widespread adoption in both academic and industrial settings. Mechanistic investigations revealed an unexpected pathway involving the photogeneration of thiyl radicals and hydrogen atoms via homolytic S–H bond cleavage under 380 nm irradiation. DFT calculations further elucidate the critical role of EtOAc in facilitating S–H bond weakening to enable light-induced homolysis. By comparison with the established photochemical approach, this convenient, efficient, and mechanistically distinct protocol offers significant versatility for the selective deuteration of formyl groups, α -amino positions, and pharmaceutically relevant compounds.

Method

General procedure for deuteration the formyl group of **1**

Under an argon atmosphere, an oven-dried 10 mL Schlenk tube equipped with a magnetic stir bar was charged with aldehyde **1** (0.2 mmol, 1.0 equiv), triisopropylsilanethiol (**thiol 1**, 2.2 μ L, 5 mol%), D₂O (160 μ L, 40 equiv), and 1.0 mL of anhydrous EtOAc solution. The mixture was degassed by the freeze-pump-thaw method, then sealed with parafilm. The solution was then stirred at room temperature under the irradiation of a 380 nm LED light for the indicated time. After completion of the reaction, the mixture was concentrated and purified by flash chromatography on silica gel.

General procedure for deuteration α -amines **3**

Under an argon atmosphere, an oven-dried 10 mL Schlenk tube equipped with a magnetic stir bar was charged with amine **3** (0.2 mmol, 1.0 equiv), triisopropylsilanethiol-d (**thiol 1-d**, 60 μ L, 30 mol%), D₂O (160 μ L, 40 equiv), methyl benzoate (13 μ L, 0.5 equiv) or methyl nicotinate (0.0137 g, 0.5 equiv), and 1.0 mL of anhydrous EtOAc solution. The mixture was degassed by the freeze-pump-thaw method, then sealed with parafilm. The solution was then stirred at 40 °C under the irradiation of a 380 nm LED light for the indicated time. After completion of the reaction, the mixture was concentrated and purified by flash chromatography on silica gel.

Data availability

Experimental procedures and characterization data are given in the Supplementary Information. The authors declare that all other data supporting the findings of this study are available within the article and its Supplementary Information files. The EPR data generated in this study have been deposited in the Science Data Bank database under accession code 10.57760/sciencedb.26334 [<https://cstr.cn/31253.11.sciencedb.26334>]. Source Data are provided with this manuscript. Source data are provided with this paper.

References

- Di Martino, R. M. C., Maxwell, B. D. & Pirali, T. Deuterium in drug discovery: progress, opportunities and challenges. *Nat. Rev. Drug Discov.* **22**, 562–584 (2023).
- Kopf, S. et al. Recent developments for the deuterium and tritium labeling of organic molecules. *Chem. Rev.* **122**, 6634–6718 (2022).
- Li, N., Li, Y., Wu, X., Zhu, C. & Xie, J. Radical deuteration. *Chem. Soc. Rev.* **51**, 6291–6306 (2022).
- Pirali, T., Serafini, M., Cargnin, S. & Genazzani, A. A. Applications of deuterium in medicinal chemistry. *J. Med. Chem.* **62**, 5276–5297 (2019).
- Başçor, R. et al. Two is better than one: deuterium in analytical mass spectrometry. *TrAC Trends Anal. Chem.* **178**, 117842 (2024).
- Lei, Z. et al. Unraveling the role of deuterium in cancer: mechanisms, detection techniques, and therapeutic potential. *Mol. Divers.* <https://doi.org/10.1007/s11030-025-11221-7> (2025).
- Liu, L., Xu, M., Xu, X., Tao, X. & Gao, Z. High sensitivity X-ray detectors with low degradation based on deuterated halide perovskite single crystals. *Adv. Mater.* **36**, 2406443 (2024).
- Cai, G. et al. Deuteration-enhanced neutron contrasts to probe amorphous domain sizes in organic photovoltaic bulk heterojunction films. *Nat. Commun.* **15**, 2784 (2024).

9. Huang, T. et al. Enhancing the efficiency and stability of blue thermally activated delayed fluorescence emitters by perdeuteration. *Nat. Photonics* **18**, 516–523 (2024).
10. Jung, S. et al. Enhancing operational stability of OLEDs based on subatomic modified thermally activated delayed fluorescence compounds. *Nat. Commun.* **14**, 6481 (2023).
11. Mullard, A. FDA approves first deuterated drug. *Nat. Rev. Drug Discov.* **16**, 305–305 (2017).
12. Hoy, S. M. Deucravacitinib: first approval. *Drugs* **82**, 1671–1679 (2022).
13. Prakash, G., Paul, N., Oliver, G. A., Werz, D. B. & Maiti, D. C–H deuteration of organic compounds and potential drug candidates. *Chem. Soc. Rev.* **51**, 3123–3163 (2022).
14. Li, W. et al. Scalable and selective deuteration of (hetero)arenes. *Nat. Chem.* **14**, 334–341 (2022).
15. Li, P., Wang, Y., Zhao, H. & Qiu, Y. Electroreductive cross-coupling reactions: carboxylation, deuteration, and alkylation. *Acc. Chem. Res.* **58**, 113–129 (2024).
16. Jedlovčnik, L. et al. Sustainable synthetic routes to deuterium-labelled organic compounds using immobilized and recyclable (bio)catalysts. *Green Synth. Catal.* **6**, 1–35 (2025).
17. Loh, Y. Y. et al. Photoredox-catalyzed deuteration and tritiation of pharmaceutical compounds. *Science* **358**, 1182–1187 (2017).
18. Zhang, M., Yuan, X. A., Zhu, C. & Xie, J. Deoxygenative deuteration of carboxylic acids with D₂O. *Angew. Chem. Int. Ed.* **58**, 312–316 (2018).
19. Li, N. et al. A highly selective decarboxylative deuteration of carboxylic acids. *Chem. Sci.* **12**, 5505–5510 (2021).
20. Li, N. et al. Highly selective single and multiple deuteration of unactivated C(sp³)-H bonds. *Nat. Commun.* **13**, 4224 (2022).
21. Xu, W. et al. Synergistic catalysis for the umpolung trifluoromethylthiolation of tertiary ethers. *Angew. Chem. Int. Ed.* **57**, 10357–10361 (2018).
22. Yan, X., Pang, Y., Zhou, Y., Chang, R. & Ye, J. Photochemical dera-cemization of lactams with deuteration enabled by dual hydrogen atom transfer. *J. Am. Chem. Soc.* **147**, 1186–1196 (2024).
23. Shi, Q. et al. Visible-light mediated catalytic asymmetric radical deuteration at non-benzylic positions. *Nat. Commun.* **13**, 4453 (2022).
24. Ramanathan, D. et al. Catalytic asymmetric deuteriosilylation of exocyclic olefins with mannose-derived thiols and deuterium oxide. *Org. Chem. Front.* **10**, 1182–1190 (2023).
25. Li, H., Shabbir, M., Li, W. & Lei, A. Recent advances in deuteration reactions†. *Chin. J. Chem.* **42**, 1145–1156 (2024).
26. Ma, P., Guo, T. & Lu, H. Hydro- and deuterio-deamination of primary amines using O-diphenylphosphinylhydroxylamine. *Nat. Commun.* **15**, 10190 (2024).
27. Dabbs, J. D. et al. Designing chemical systems for precision deuteration of medicinal building blocks. *Nat. Commun.* **15**, 8473 (2024).
28. Xu, Y. et al. Selective monodeuteration enabled by bisphosphonium catalyzed ring opening processes. *Nat. Commun.* **15**, 9366 (2024).
29. Sun, K. et al. Energy-transfer-enabled photocatalytic transformations of aryl thianthrenium salts. *Nat. Commun.* **15**, 9693 (2024).
30. Vang, Z. P., Hintzsche, S. J. & Clark, J. R. Catalytic transfer deuteration and hydrodeuteration: emerging techniques to selectively transform alkenes and alkynes to deuterated alkanes. *Chem. Eur. J.* **27**, 9988–10000 (2021).
31. Bu, F. et al. Electrocatalytic alkene hydrogenation/deuteration. *J. Am. Chem. Soc.* **147**, 5785–5795 (2025).
32. Ou, W., Qiu, C. & Su, C. Photo- and electro-catalytic deuteration of feedstock chemicals and pharmaceuticals: a review. *Chin. J. Catal.* **43**, 956–970 (2022).
33. Zhou, R., Ma, L., Yang, X. & Cao, J. Recent advances in visible-light photocatalytic deuteration reactions. *Org. Chem. Front.* **8**, 426–444 (2021).
34. Ahmed Laskar, A. & Younus, H. Aldehyde toxicity and metabolism: the role of aldehyde dehydrogenases in detoxification, drug resistance and carcinogenesis. *Drug Metab. Rev.* **51**, 42–64 (2019).
35. Guo, Y. et al. Advances in C1-deuterated aldehyde synthesis. *Coord. Chem. Rev.* **463**, 214525 (2022).
36. Geng, H. et al. Practical synthesis of C1 deuterated aldehydes enabled by NHC catalysis. *Nat. Catal.* **2**, 1071–1077 (2019).
37. Dong, J.-Y. et al. Visible-light-mediated deuteration of aldehydes with D₂O via polarity-matched reversible hydrogen atom transfer. *Tetrahedron* **82**, 131946 (2021).
38. Zhang, Y., Ji, P., Dong, Y., Wei, Y. & Wang, W. Deuteration of formyl groups via a catalytic radical H/D exchange approach. *ACS Catal.* **10**, 2226–2230 (2020).
39. Dong, J. et al. Formyl-selective deuteration of aldehydes with D₂O via synergistic organic and photoredox catalysis. *Chem. Sci.* **11**, 1026–1031 (2020).
40. Kuang, Y. et al. Visible light driven deuteration of formyl C–H and hydridic C(sp³)-H bonds in feedstock chemicals and pharmaceutical molecules. *Chem. Sci.* **11**, 8912–8918 (2020).
41. Xu, Q. et al. Photosynthesis of C-1-deuterated aldehydes via chlorine radical-mediated selective deuteration of the formyl C–H bond. *Org. Lett.* **26**, 4098–4103 (2024).
42. Meng, X., Che, C., Dong, Y., Liu, Q. & Wang, W. Organophotocatalytic selective deuteration of metabolically labile heteroatom adjacent C–H bonds via H/D exchange with D₂. *Org. Lett.* **26**, 8961–8966 (2024).
43. Meng, X., Dong, Y., Liu, Q. & Wang, W. Organophotocatalytic α-deuteration of unprotected primary amines via H/D exchange with D₂O. *Chem. Commun.* **60**, 296–299 (2024).
44. Legros, F. et al. Photoredox-mediated hydrogen isotope exchange reactions of amino-acids, peptides, and peptide-derived drugs. *Chem. Eur. J.* **26**, 12738–12742 (2020).
45. Dénès, F., Pichowicz, M., Povie, G. & Renaud, P. Thiyl radicals in organic synthesis. *Chem. Rev.* **114**, 2587–2693 (2014).
46. Qiao, B. et al. Single-atom catalysis of CO oxidation using Pt₁/FeO_x. *Nat. Chem.* **3**, 634–641 (2011).
47. Itoh, T. The lowest excited triplet (T₁) energies of p-methoxybenzaldehyde and p-cyanobenzaldehyde vapors estimated from the temperature dependence of the T₂(n, π*) phosphorescence and the S₁(n, π*) fluorescence spectra. *Spectrochim. Acta A Mol. Biomol. Spectrosc.* **59**, 61–68 (2003).
48. Wang, J. et al. Depolymerization of native lignin over thiol capped ultrathin ZnIn₂S₄ microbelts mediated by photogenerated thiyl radical. *Angew. Chem. Int. Ed.* **63**, e202410397 (2024).
49. Peng, J. et al. Photocatalytic generation of hydrogen radical (H•) with GSH for photodynamic therapy. *Angew. Chem. Int. Ed.* **62**, e202214991 (2023).
50. Chen, L. et al. Accurate identification of radicals by in-situ electron paramagnetic resonance in ultraviolet-based homogenous advanced oxidation processes. *Water Res.* **221**, 118747 (2022).
51. Qin, L., Huang, C.-H., Mao, L., Shao, B. & Zhu, B.-Z. First unequivocal identification of the critical acyl radicals from the anti-tuberculosis drug isoniazid and its hydrazide analogs by complementary applications of ESR spin-trapping and HPLC/MS methods. *Free Rad. Biol. Med.* **154**, 1–8 (2020).
52. Luo, Y.-R. *Comprehensive Handbook of Chemical Bond Energies* (CRC Press, 2007).
53. Zhou, R. et al. Visible-light-mediated metal-free hydrosilylation of alkenes through selective hydrogen atom transfer for Si–H activation. *Angew. Chem. Int. Ed.* **56**, 16621–16625 (2017).
54. Surdhar, P. S. & Armstrong, D. A. Reduction potentials and exchange reactions of thiyl radicals and disulfide anion radicals. *J. Phys. Chem.* **91**, 6532–6537 (2002).
55. Hernandez-Perez, A. C. & Collins, S. K. A visible-light-mediated synthesis of carbazoles. *Angew. Chem. Int. Ed.* **52**, 12696–12700 (2013).

56. Seo, E. T. et al. Anodic oxidation pathways of aromatic amines. Electrochemical and electron paramagnetic resonance studies. *J. Am. Chem. Soc.* **88**, 3498–3503 (2002).
57. Adenier, A., Chehimi, M. M., Gallardo, I., Pinson, J. & Vilà, N. Electrochemical oxidation of aliphatic amines and their attachment to carbon and metal surfaces. *Langmuir* **20**, 8243–8253 (2004).

Acknowledgements

Financial support for this work was provided by the National Natural Science Foundation of China (22271261, Z.W.); the Natural Science Foundation of Henan Province (232300421365, Y.Z.); the National Natural Science Foundation of China (22107045 and 82472934, Z.Z.); the Hospital Fund of National Cancer Center/National Clinical Research Center for Cancer/Cancer Hospital & Shenzhen Hospital, Chinese Academy of Medical Sciences and Peking Union Medical College, Shenzhen (E010221005 and CFA202201006, Z.Z.).

Author contributions

Z.W. and Y.Z. designed and guided this project. Y.M., B.S. and J.Z. conducted the experiments and analyzed the data. Z.Z. conducted a DFT calculation. W.W., H.R., Y.Z., K.L., Z.L. and Z.W. discussed the results. Y.Z. and Z.W. wrote the manuscript. All authors discussed comments on the manuscript.

Competing interests

The authors declare no competing interests.

Additional information

Supplementary information The online version contains supplementary material available at <https://doi.org/10.1038/s41467-025-61641-0>.

Correspondence and requests for materials should be addressed to Zhiyuan Wang or Yueteng Zhang.

Peer review information *Nature Communications* thanks Qingmin Wang and the other, anonymous, reviewers for their contribution to the peer review of this work. A peer review file is available.

Reprints and permissions information is available at <http://www.nature.com/reprints>

Publisher's note Springer Nature remains neutral with regard to jurisdictional claims in published maps and institutional affiliations.

Open Access This article is licensed under a Creative Commons Attribution-NonCommercial-NoDerivatives 4.0 International License, which permits any non-commercial use, sharing, distribution and reproduction in any medium or format, as long as you give appropriate credit to the original author(s) and the source, provide a link to the Creative Commons licence, and indicate if you modified the licensed material. You do not have permission under this licence to share adapted material derived from this article or parts of it. The images or other third party material in this article are included in the article's Creative Commons licence, unless indicated otherwise in a credit line to the material. If material is not included in the article's Creative Commons licence and your intended use is not permitted by statutory regulation or exceeds the permitted use, you will need to obtain permission directly from the copyright holder. To view a copy of this licence, visit <http://creativecommons.org/licenses/by-nc-nd/4.0/>.

© The Author(s) 2025